RSC Advances

ROYAL SOCIETY OF CHEMISTRY

www.rsc.org/advances

Dihydroisoquinoline Copper(II) Complexes: Crystal Structures, Cytotoxicity, and Their Action Mechanism

Ke-Bin Huang,[a,b] Zhen-Feng Chen,[a]* Yan-Cheng Liu,[a] Xiao-Li Xie,[a] and Hong Liang[a,b]*

Received (in XXX, XXX) Xth XXXXXXXXX 20XX, Accepted Xth XXXXXXXXX 20XX
DOI: 10.1039/b000000x

Three new copper(II) complexes of 4,5-methylenedioxy-1-pyridinedihydroisoquinoline (MPDQ), $[Cu_2(MPDQ)_2Cl_4]$ (**1**), $[Cu(MPDQ)(H_2O)(SO_4)]$ (**2**), and $[Cu_2(MPDQ)_2(C_2O_4)(ClO_4)_2]$ (**3**) were synthesized and characterized. They exhibit enhanced cytotoxicity against the tested human tumor cells BEL-7404, SK-OV-3, HepG2, A549, A375, MGC-803 and NCI-H460 with IC_{50} values of 1.41~34.54 μM in comparing to MPDQ and corresponding copper(II) salts. Complex **1** can induce BEL-7404's apoptotic death by S cell cycle arrest, and complex **1** induced apoptosis which were involved in intrinsic pathway by up-regulating P53, down-regulating Bcl-2 and mitochondrial membrane potential, leading to sequential activation of the Caspase-9, Caspase-3. ICP-MS testing implied that the copper(II) complexes could enter cells and DNA was one important target; DNA binding studies revealed that the intercalation might be the most possible binding mode of the new Cu(II) complexes with ct-DNA.

Introduction

Cisplatin is a widely used and well-known metal-based drug for cancer therapy, but it possesses inherent side effects and low administration dosage has to be used.[1-3] Therefore, increasing efforts are being made to improve this drug with suitable alternatives, and numerous non-platinum-based antitumor complexes are synthesized and screened for their anticancer activities.[4-9] In addition to the Ru(II) complexes, Cu(II) complexes are regarded as the best alternatives to replace cisplatin as anticancer agents.[9-11] Copper is known to play a significant role in biological systems and it also has been used as a pharmacological agent.[12-14] Synthetic copper(II) complexes have been reported to act as potential anticancer agents, and a number of copper complexes have been found to be active in vivo.[15-17]

Isoquinolines, a type of alkaloids, are widespread in nature and they exhibit a variety of biological activities, including inhibition of cellular proliferation and cancer development.[18-21] For example, berberrubine, a protoberberine alkaloid, showed antitumor activity in animal models,[22] and 6-Alkyl-12-formyl-5,6-dihydroindolo-[2,1-a]-isoquinolines have been also shown to inhibit the growth of human mammary cells.[23-24] Since the broad biological effects of isoquinolines, during the past two decades, a series of isoquinoline and related platinum(II) complexes with potent anticancer activity have been reported by Steglich and Farrell et al.[25-27] Previous studies from our group revealed that the transition metal complexes of natural isoquinolines alkaloids, including the active ingredient liriodenine and oxoglaucine in traditional Chinese medicines, also exhibited promising anticancer activity.[7,29-31] 3,4-dihydroisoquinoline (thalpetaline) was isolated from the EtOH-ext. of the Chinese medicinal herb T. petaloideum known for its diarrhea, hepatitis, skin infections and anticancer efficency,[32] which is a good leading compound widely applied to design new antitumor agents.[33-35] Recently, we have utilized 3,4-dihydroisoquinoline as the leading compound to design and synthesize one isoquinoline derivative, 4,5-methylenedioxy-1-pyridinedihydroisoquinoline (MPDQ), which contains DNA intercalation moiety and pyridine ring, can be acted as chelating ligand (Scheme 1), and the antitumor activity of the Zn(II)/Ni(II) complexes have been also reported for the MPDQ ligand.[36] As a part of our research for new metal based anticancer agents, herein, we report the synthesis, crystal structure and in vitro antitumor activity of three copper(II) complexes with MPDQ as chelating ligand, and the mechanism of their cytotoxicity as well as their interactions with the potential target DNA were also investigated.

Experimental

Materials and reagents

All chemicals, unless otherwise noted, were purchased from Sigma and Alfa Aesar. All materials were used as received without further purification unless noted specifically. Tris-HCl-NaCl (TBS) buffer solution (5 mM Tris, 50 mM NaCl, pH adjusted to 7.35 by titration with hydrochloric acid using a Sartorius PB-10 pH meter, Tris = tri(hydroxymethyl)aminomethane) was prepared using double distilled water. The TBE buffer (1 ×) and DNA loading buffer (6 ×) were commercially available. Calf thymus DNA (ct-DNA) was purchased from Sino-American Biotech Co., Ltd. (Beijing, China). Ct-DNA gave a UV absorbance ratio at 260−280 nm of ~1.85:1, indicating that the DNA was effectively free of protein. The DNA concentration per nucleotide was determined spectrophotometrically by employing a molar absorption coefficient (6600 $M^{-1}cm^{-1}$) at 260 nm. The stock solution of pUC19 plasmid DNA (250 μg/mL) was purchased from Takara

Biotech Co., Ltd.

Instrumentation

^{1}H NMR and ^{13}C NMR spectra were recorded on a Bruker AV-600 NMR spectrometer with DMSO-d^6 as solvent. Elemental analyses (C, H, and N) were carried out on a PerkinElmer Series II CHNS/O 2400 elemental analyzer. ESI-MS spectra for the characterization of the complexes were performed on a Bruker HCT Electro spray Ionization Mass Spectrometer.

Table1 Crystal data and structure refinement details for complexes **1–3**

Formula	$C_{30}H_{24}C_{l4}Cu_2N_4O_6$	$C_{15}H_{14}CuN_2O_7S$	$C_{16}H_{12}ClCuN_2O_8$
fw	781.22	429.90	459.27
T / K	293(2)	293(2)	293(2)
crystal system	Triclinic	Orthorhombic	Monoclinic
space group	P-1	Pbca	P21/c
a, Å	7.6582 (3)	7.3674(1)	7.8720(4)
b, Å	8.8071 (4),	18.0273(3)	17.1458(5)
c, Å	11.4566 (8)	23.5080(4)	12.8986(5)
α, º	97.269 (5)	90.00	90.00
b, Å	101.942 (5)	90.00	102.085(5)
γ, º	108.179 (4)	90.00	90.00
V, Å^3	702.91 (6)	3122.20(9)	1702.35(12)
Z	1	8	4
D_c, g cm^{-3}	1.846	1.769	1.792
μ, mm^{-1}	1.94	1.58	1.492
GOF on F^2	1.01	1.06	1.068
Reflns(collected/unique)	3194/199	11090/ 3236	17371/3478
R_{int}	0.023	0.021	0.0483
R_1[a] ($I > 2\sigma(I)$)	0.0349	0.0266	0.0403
wR_2[b] (all data)	0.0849	0.0718	0.0849

[a] $R_1 = \Sigma ||F_o| - |F_c||/\Sigma|F_o|$; [b] $wR_2 = [\Sigma w(F_o^2 - F_c^2)^2/\Sigma w(F_o^2)$

Synthesis of the copper(II) complexes

4,5-Methylenedioxy-1-pyridinedihydroisoquinoline (MPDQ) was synthesized according to previous reported methods.[37]

General procedures for the synthesis of complexes **1**−**3**. To a mixture of the corresponding metal salt, 4,5-methylenedioxy-1-pyridinedihydroisoquinoline (MPDQ), methanol (1 mL), and $CHCl_3$ (0.5 mL) was placed in a thick Pyrex tube (~20 cm long). The mixture was frozen by liquid N_2 and evacuated under vacuum, then sealed with a torch, warmed to room temperature, and heated at 110 °C for several days to give the corresponding block crystals of complexes **1**−**3** suitable for X-ray diffraction analysis.

Complex **1**: $CuCl_2{\cdot}H_2O$ (0.015 g, 0.1 mmol), MPDQ (0.050 g, 0.2 mmol). Yield 65%. Anal. Found (%): C, 46.59; H, 3.13; N, 7.24. Calcd for: C, 45.98; H, 3.37; N, 7.16. ESI-MS: m/z 349.9 $[Cu(MPDQ)Cl]^+$.

Complex **2**: $CuSO_4{\cdot}5H_2O$ (0.025 g, 0.1 mmol), MPDQ (0.050 g, 0.2 mmol). Yield 70%. Anal. Found(%): C, 41.91; H, 3.28; N, 6.52. Calcd for: C, 42.08; H, 3.21; N, 6.48. ESI-MS: m/z 412.4 $[Cu(MPDQ)SO_4]^+$.

Complex **3**: $Cu(ClO_4)_2{\cdot}6H_2O/(COOK)_2{\cdot}H_2O$ (0.037 g/0.018 g, 0.1 mmol/0.1 mmol), MPDQ (0.050g, 0.2 mmol). Yield 63%. Anal. Found (%): C, 41.84; H, 2.63; N, 6.10. Calcd for: C, 41.92; H, 2.58; N, 6.17. ESI-MS: m/z 466.0 $[Cu(MPDQ)ClO_4{+}H_2O + CH_3OH]^+$.

X-ray crystallographic analysis

All reflection data were collected on Agilent Super Nova diffractometer by using graphite-monochromatic Mo-Kα radiation (λ = 0.71073 Å) at room temperature. The crystal structures were solved by the direct method using the program SHELXS-97 [38] and refined by the full-matrix least-squares method on F^2 for all non-hydrogen atoms using SHELXL-97[39] with anisotropic thermal parameters. All hydrogen atoms were located in calculated positions and refined isotropically, except the hydrogen atoms of water molecules were fixed in a difference Fourier map and refined isotropically. The crystallographic data and refinement details of the structures are summarized Table 1.

Cell lines, culture conditions and cytotoxicity assay

Human tumor cells BEL-7404, SK-OV-3, A549, A375, MGC-803 and NCI-H460 were obtained from the Shanghai Cell Bank in the Chinese Academy of Sciences. The tumor cells were grown in the RPMI-1640 medium supplemented with 10% (v/v) fetal bovine serum, 2 mM glutamine, 100 U/mL penicillin, and 100 U/mL streptomycinin at 37 °C, in a highly humidified atmosphere of 95% air/5% CO_2. The cytotoxicity of the title complexes against BEL-7404, SK-OV-3, A549, A375, MGC-803, NCI-H460 cells were examined by the micro culture tetrozolium (MTT) assay. The experiments were carried out using reported procedure.[40] The growth inhibitory rate of the treated cells was calculated using the data from three replicate tests as $(OD_{control} - OD_{test})/OD_{control} \times 100\%$. The complexes were incubated with various cells for 48 h at five different concentrations of the complexes dissolved in fresh media; the range of concentrations

used was dependent on the complexes. The final IC_{50} values were calculated by the Bliss method (n = 5). All tests were independently repeated at least three times.

Uptake of copper(II) complex in BEL-7404 and in nuclear DNA

The cells were seeded in Petridish. After 24 h of pre-incubation time in drug-free medium at 37 °C in a humidified atmosphere of 5% CO_2/95% air, the complex **1** were added to give final concentrations at 10, 20 μM. After a further 24 h of drug exposure, cells pellets were digested with HNO_3, the resulting solutions were diluted with double-distilled water to a final concentration of 5% HNO_3 (5 mL), and the copper contents was determined by plasma-mass spectrometry (ICP-MS). Data is the mean of three experiments and reported as mean ± SD.[36]

The cells were seeded in 6-well tissue culture plates for 24 h, and then treated with complex **1** at 10, 20 μM. After 24 h incubation, cells were washed three times with ice cold PBS (1-2 mL). The genomic DNA was extracted according to QIAamp DNA Mini Kit (50). Each DNA sample was digested with HNO_3, the resulting solutions were diluted with double-distilled water to a final concentration of 5% HNO_3 (5 mL), and the copper contents were determined by ICP-MS. Data is the mean of three experiments and reported as mean ± SD.[36]

Apoptosis assay by flow cytometry

The ability of copper complex **1** to induce apoptosis was evaluated in BEL-7404 cell lines using Annexin-V conjugated with FITC and propium iodide (PI) counter staining by flow cytometry. BEL-7404 cells of exponential growth were incubated in 6-well plates and cultured for 12 h before the tested compounds were added to give the indicated final concentrations. After 48 h incubation, cells were harvested, washed twice in phosphate-buffered saline (PBS), and resuspended in 100 μL binding buffer (including 140 mmol/L NaCl, 2.5 mmol/L $CaCl_2$ and 10 mmol/L Hepes / NaOH, pH 7.4) at a concentration of 1×10^6 cells/mL. Then the cells were incubated with 5 μL of Annexin V- FITC (in buffer including 10 m mol/L NaCl, 1% bovine serum albumin, 0.02% NaN_3 and 50 mmol/L Tris, pH 7.4) and 10 μL PI (20 μg/mL) for 15 min at room temperature in the dark. Cells were kept shielded from light before being analyzed by flow cytometry using a Becton-Dickinson FACSC alibur.

Apoptosis assay by confocal microscopy

BEL-7404 cells were grown on chamber slides to 70% confluence. Complex **1** (0.5 μM) was added to the culture medium (final DMSO concentration, 5 % v/v) and incubated for 12 h at 37 °C. The cells were then washed with PBS, stained with medium containing DAPI/DiD solution (100 mg/mL DAPI, 100 mg/mL DiD) for 30 min, photographed with a Zeiss LSM7.

Cell cycle analysis

BEL-7404 cell lines were maintained in Dulbecco's modified Eagle's medium with 10 % fetal calf serum in 5 % CO_2 at 37 °C. Cells were harvested by trypsinization and rinsed with PBS. After centrifugation, the pellet (10^5–10^6 cells) was suspended in 1 mL of PBS and kept on ice for 5 min. The cell suspension was then fixed by the dropwise addition of 9 mL pre-cooled (4 °C) 100% ethanol with violent shaking. Fixed samples were kept at 4 °C until use. For staining, cells were centrifuged, resuspended in PBS, digested with 150 mL of RNase A (250 mg/mL), and treated with 150 mL of propidium iodide (PI) (0.15 mM), then incubated for 30 min at 4 °C. PI-positive cells were counted with a FACScan Fluorescence-activated cell sorter (FACS). The population of cells in each cell cycle phase was determined using Cell Modi FIT software (Becton Dickinson).

Determination of caspase-3 activity

The activation of caspase-3 was examined using a caspase-3 (DEVD-FMK) conjugated to FITC as the fluorescent in situ marker in living cells (catalog#QIA91, Merk). FITC-DEVD-FMK is cell permeable, nontoxic, and irreversibly binds to activated caspase-3 in apoptotic cells. After exposure of BEL-7404 cell lines to complex **1** for 4 h, the cultures were washed twice with HBSS containing 0.1% BSA and then incubated with FITC-DEVD-FMK (1 μl/ml in EBSS) for 1 h in a 37 ºC incubator with 5% CO_2. The FITC label in apoptotic cells was examined immediately under fluorescent microscope with excitation and emission at 485 and 535 nm, respectively.

Mitochondrial membrane potential detection

Cells incubated with the IC_{50} concentration of complex **1** for 12 h in poly-HEMA coated 6-wells were collected and resuspended in fresh medium. After the addition of 0.5 mL JC-1 working solution, the cells were incubated in a 5 % CO_2 incubator for 20 min at 37 °C. The staining solution was removed by centrifugation and cells were washed with JC-1 staining buffer twice. Cells having low membrane potential were taken pictures under fluorescent microscope (120×).

Western blotting

BEL-7404 cells (5×10^5) were cultured on 60 mm dish and incubated overnight before experiments, which were treated with complex **1** at concentration of 5 μM for 12, 24, 36 h. After incubation, cells were harvested and lysed using the lysis buffer (150 mM NaCl, 100 mM Tris-HCl, pH 7.4, 10% glycerol, 1% Triton X-100, 10 mM NaF, 5 mM sodium pyrophosphate, 5 mM sodium orthovanadate, 0.1% SDS) with protease inhibitor. Total protein extracts (50 μg) were loaded onto suitable concentration SDS-polyacrylamide gel, and were then transferred to polyvinylidene fluoride (PVDF) membranes. The membrane was blocked with 5% BSA in TBST buffer and incubated with corresponding primary antibodies at 4 ºC overnight, P-53 (ab17990, 1:500), Bcl-2 (ab32124) (1:2000), cleaved caspase-3 (ab32042) (1:500), cleaved caspase-9 (ab32539) (1:500) were obtained from Abcam. After washing, the membrane was incubated with secondary antibody conjugated with horseradish peroxidase (1:2500) for 120 min. The immuno reactive signals were detected using enhanced chemoluminance kit (Pierce ECL Western Blotting Substrate) following the procedures given in the user manual.

DNA binding studies

The 2×10^{-3} M ct-DNA stock solution was stored at 4 °C for no more than 5 days before use. The synthetic copper(II) complexes were all prepared as 2×10^{-3} M DMSO stock solutions for DNA binding studies. The final working solutions of the complexes for

DNA binding studies were diluted by TBS and the DMSO containing was less than 10 %. A solution containing 2×10^{-4} M DNA and 2×10^{-5} M EB ([DNA]/[EB] = 10:1) was prepared for EB-ct-DNA competitive binding studies. The melting temperatures of DNA and the DNA−complexes were determined by monitoring the absorbance at 260 nm of the samples at different temperatures. The absorbance intensities were then plotted as a function of the temperature ranging from 25 to 95 °C. The values of melting temperatures of DNA and the DNA−complexes were obtained from the transition midpoint of the melting curves based on fss versus temperature (T), where fss = $(A-A_0)/(A_f - A_0)$, where A_0 is the initial absorbance intensity, A is the absorbance intensity corresponding to its temperature, and A_f is the final absorbance intensity.[41] Fluorescence emission spectra were recorded under slit width as 10 nm/10 nm for E_x/E_m, respectively. The quenching constant for comparing the efficiency of fluorescence quenching, i.e., K_q of each compound was obtained by the linear fit of plotting I_0/I versus [Q], according to the classic Stern–Volmer equation: $I_0/I = 1+K_q\times[Q]$,[42] where I_0 and I are the peak emission intensity of the EB-ct-DNA system in the absence and presence of each compound as quencher, and [Q] is the concentration of quencher. CD absorption spectra of DNA were measured in TBS at a 100 nm/min scan rate in the wavelength range from 200 to 400 nm, with 1×10^{-4} M DNA in the absence and presence of each compound of 2×10^{-5} M, respectively. The CD signal of TBS was taken as the background and subtracted from the spectra. All the spectroscopic experiments were performed at 25 °C. In DNA viscosity measurements, ct-DNA was dissolved in BPE buffer (6 mM Na_2HPO_4, 2 mM NaH_2PO_4, 1mM Na_2EDTA, pH ¼ 7.2) to prepare a 8 $x10^{-4}$ M working solution. The compounds were added until reaching the desired [compound]/[DNA] ratios ranging from 0.02 to 0.20 in every 0.02 interval. The circulating bath temperature was maintained at 35.0±0.1 °C. The viscosities η (unit: cP) were directly obtained by running spindle in the working samples at 30 rpm. The data were presented as η/η_0 versus [compound]/[DNA] ratio, in which η_0 and η refer to the viscosity of the DNA working solutions in the absence and presence of the corresponding compound, respectively. The influences of solvent DMSO on the viscosity were eliminated by subtracting its viscosity 2.03 cP (measured at 35.0 °C) from the sample viscosities.

Statistics

The data processing included the Student's t-test with $P \le 0.05$ taken as significance level, using SPSS 13.0.

Results and discussion

Synthesis

The isoquinoline ligand MPDQ was prepared according to the method reported in our prior study, which was synthesized by Bischler-Napieralski cyclization of the acylation product (ALP) of phomopiperonylamine and picolinic acid (Scheme 1).[37]

Jan Reedijk's works indicated that metal complexes with different anions and identical ligand had different bioactivities,[43] here, the present three Cu(II) complexes $[Cu_2(MPDQ)_2Cl_4]$ (**1**), $[Cu(MPDQ)(H_2O)(SO_4)]$ (**2**), and $[Cu_2(MPDQ)_2(C_2O_4)(ClO_4)_2]$ (**3**) were obtained by treating MPDQ with $CuCl_2.2H_2O$,with $CuCl_2.2H_2O$, $CuSO_4.5H_2O$, $Cu(ClO_4)_2.6H_2O/(COOK)_2{\cdot}H_2O$ (1:1) in $CH_3OH/CHCl_3$ (2:1) under the solvothermal conditions.

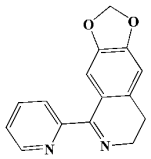

MPDQ

Scheme 1 isoquinoline ligand MPDQ

The products were characterized by elemental analysis, ESI-MS spectra and single crystal X-ray diffraction analysis.

Structure description and stability in solution

The molecular structures of the three complexes $[Cu_2(MPDQ)_2Cl_4]$ (**1**), $[Cu(MPDQ)(H_2O)(SO_4)]$ (**2**), and $[Cu_2(MPDQ)_2(C_2O_4)(ClO_4)_2]$ (**3**) are depicted in Figs. 1–3. Complexes **1** and **3** are binuclear structures, whereas complex **2** is a one-dimensional chain structure. As shown in Fig. 1, the two Cu(II) centers in complex **1** are bridged by two chloride anions. Each Cu(II) centre adopts a distorted square pyramid geometry by coordinating with one Cl, two μ_2-Cl, and two N atoms from MPDQ. As shown Fig. 2, the Cu(II) centre in complex **2** adopts a distorted square planar geometry by coordinating with one aqua, one O atom from μ_2-SO_4^{2-} anion, and two nitrogen atoms from MPDQ. By means of μ_2-SO_4^{2-} linking two adjacent copper(II) centers, a one-dimensional chain structure is formed. Complex **3** is a dinuclear structure, in which the $[Cu(MPDQ)(ClO_4)]^+$ is bridged by one tetra-dentate oxalate anion, the Cu(II) centre adopts a distorted square pyramid geometry by coordinating with one O from ClO^{4-}, two oxygen from oxalate anion, and two nitrogen from MPDQ. Similarly, two chlorine atoms in complex **1** and two perchlorates in complex **2** lie in the opposite sides of the plane formed by bridged μ_2-Cl or oxalate and two copper(II) centers. As the reported $[Zn_2(L)_2(\mu_2\text{-}Cl)_2Cl_2]$ complex,[37] the ESI-MS results show that the chlorine bridge of complex **1** is broken in a polar solution system (DMSO, methanol, H_2O) and exists in a mononuclear form, $[CuCl(MPDQ)]^+$ (ESI-MS: m/z $[CuCl(MPDQ)]^+$ =349.9). As complex **1**, complexes **2**, **3** have also been dissociated into a mononuclear form in a polar solution system (DMSO, methanol, H_2O), ESI-MS: m/z 412.4 $[Cu(MPDQ)Cl]^+$ (for complex **2**), and m/z 466.0 $[Cu(MPDQ)ClO_4{+}H_2O{+}CH_3OH]^+$ (for complex **3**). The stabilities of Cu complexes were investigated under physiological conditions (Tris-KCl-HCl buffer Solution with pH value of 7.35, containing 1% DMSO) by the mean of HPLC. As shown in Fig. S1 (Supporting Information), the time-dependent (at 0, 24, and 48 h) HPLC spectra of each complex indicated that the present Cu(II) complexes were stable in TBS (Tris-KCl-HCl) buffer solution for 48 h at room temperature.

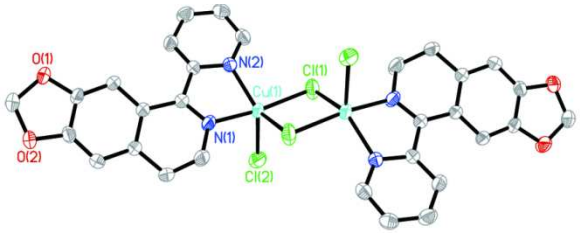

Fig. 1. ORTEP drawing of complex **1**. The hydrogen atoms have been omitted for clarity. Selected bond lengths (Å) and angles (°) for complex **1**: Cu(1)–N(1) 1.9713(22), Cu(1)–N(2) 2.0433(20), Cu(1)–Cl(1) 2.2718(7), Cu(1)–Cl(2) 2.3480(8), N(1)–Cu(1)–N(2) 78.87(8), Cl(1)–Cu(1)–N(1) 70.69(8), Cl(2)–Cu(2)–N(1), 92.06(8), N(2)–Cu(1)–Cl(1) 96.17(6), N(2)–Cu(1)–Cl(2) 122.61(6), Cl(1)–Cu(1)–Cl(2) 97.25(3).

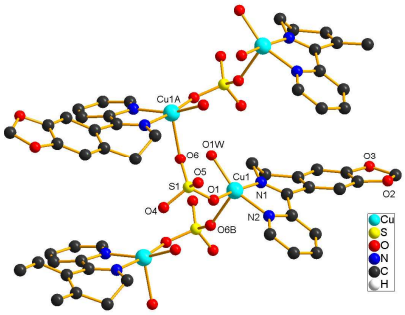

Fig. 2. ORTEP drawing of complex **2**, and the hydrogen atoms have been omitted for clarity. Selected bond lengths (Å) angles (°), for complex **2**: Cu(1)–O(1w) 1.9576(15), Cu(1)–O(1) 1.9620(14), Cu(1A)–O(6) 2.2221(15), Cu(1)–N(1) 1.9648 (17), Cu(1)–N(2) 1.9944(17); O(1)–Cu(1)–O(1w) 93.81(6), N(1)–Cu(1)–O(1w) 91.83(7), N(2)–Cu(1)–O(1w) 159.85(7), N(1)–Cu(1)–O(1) 172.25 (7), N(2)–Cu(1)–O(1) 92.32(7), N(2)–Cu(1)–N(1) 80.62(7). (Symmetry code A: 1/2+x, 1/2−y, −z; B: −1/2+x, 1/2−y, −z)

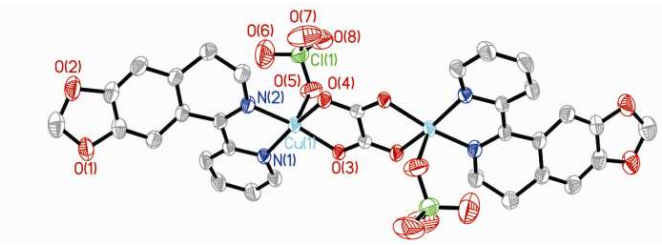

Fig. 3. ORTEP drawing of complex **3**, and the hydrogen atoms have been omitted for clarity. Selected bond lengths (Å) angles (°): Cu(1)–N(1) 1.9693(23), Cu(1)–N(2) 1.9483(25), Cu(1)–O(3) 1.9744(19), Cu(1)–O(4) 1.9917(19), Cu(1)–O(5) 2.2616(27), N(1)–Cu(1)–N(2) 82.27(10), O(3)–Cu(1)–N(2) 169.66(10), O(4)–Cu(2)–N(2) 95.80(9), O(5)–Cu(1)–N(2) 103.60(11), N(1)–Cu(1)–O(3) 95.04(9), N(1)–Cu(1)–O(4) 166.73(11), N(1)–Cu(1)–O(5) 96.51(11), O(3)–Cu(1)–O(4) 84.52(8), O(3)–Cu(1)–O(5) 86.60(9), O(4)–Cu(1)–O(5) 96.70(10).

In vitro cytotoxic activity

The in vitro cytotoxicity of MPDQ and complexes **1**–**3** against BEL-7404, SK-OV-3, A549, A375, MGC-803, NCI-H460 and HL-7702 cell lines were investigated (cisplatin as the positive control). As shown in Table 2, towards the tested cells, the IC_{50} exhibited significantly enhanced activities compared to that of free MPDQ and the corresponding copper(II) salts, suggesting synergistic effect between MPDQ and copper(II) ions. It should be noted that these copper(II) complexes towards the normal human liver HL-7702 cells displayed lower cytotoxicity than that of them to the tested cancer cells, thereby, complexes **1**–**3** exhibited a certain extent selectivity to cancer cells. Among them, complex **1** against BEL-7404, A549, A375 exhibited the highest cytotoxicity with the IC_{50} values of 1.41~3.34 μM. Complex **3** against BEL-7404, A549 and MGC-803 also exhibited higher cytotoxicity with the IC_{50} values of 3.39~6.32 μM. Based on their structures and the molecular species in solution (ESI-MS data), it could be envisioned that the approximately planar benzo[1,3]dioxole moiety of MPDQ that can intercalate between adjacent base pairs of DNA, together the copper ion played a key role in their cytotoxicity.[31] Since complex **1** displayed the highest cytotoxicity in most cases, it was used as a representative compound in the following studies on the mechanism of cell cytotoxicity against the BEL-7404 cancer cell.

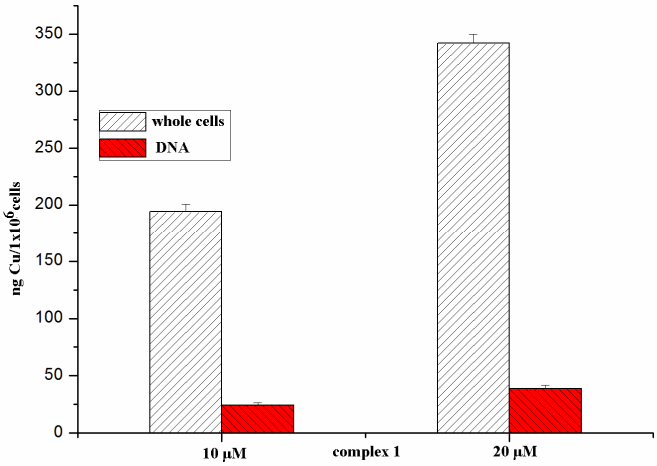

Fig. 4. The uptake and DNA accumulation of copper element determined in BEL-7404 cells after 48 h of exposure to 10/20 μM of complex **1**

The uptake of copper(II) complex in BEL-7404 cells and nuclear DNA

The cellular uptake properties of metal-based anticancer drugs are important factors that can influence their antiproliferative efficacies. To investigate if copper complex enter cells, we have determined copper uptake of complex **1** (having lower IC_{50} values) in BEL-7404 cells by ICP-MS. Cells were treated with complex **1** at 10, 20 μM for 24 h, the accumulation of metal copper in the 10^6 cells were 1940 ng and 3427 ng, respectively (see Fig. 4.). The results indicated that the complex **1** could translate cell membrane well.

Table 2 IC_{50} (μM) values for complexes **1–3** against six human tumor cell lines

Complexes	BEL-7404	SK-OV-3	A549	A375	MGC-803	NCI-H460	HL-7702
MPDQ	38.41±0.27	67.58±4.87	31.55±3.46	37.67±2.39	55.41±1.58	>100	>100
1	3.34±0.51	18.27±0.14	1.41±0.25	2.38±0.04	14.57±2.11	34.54±3.07	20.78±0.09
2	11.25±0.21	24.76±0.32	14.24±0.18	8.29±0.22	7.48±0.34	24.81±1.25	68.52±0.06
3	4.12±0.07	17.33±0.41	6.32±0.08	11.57±0.36	3.39±0.06	17.23±0.78	28.66±0.16
$CuCl_2.2H_2O$	74.38±5.68	ND[b]	81.31±2.17	60.26±3.04	72.15±3.17	41.07±1.54	>100
$CuSO_4.5H_2O$	>100	ND[b]	ND[b]	>100	>100	82.44±3.37	70.10±0.06
$Cu(ClO_4)_2.6H_2O$	63.26±4.14	ND[b]	87.54±6.22	69.13±1.12	52.24±2.29	53.19±4.10	>100
cisplatin[a]	64.22±1.21	84.21±0.24	17.21±0.58	78.54±2.25	23.58±0.43	48.52±0.32	74.25±0.11

[a]Cisplatin was used as positive control. [b]ND is no data.

To verify supposition that DNA may be one important target for the complexes, the copper contents of complex **1** in DNA sample which was isolated have been examined by ICP-MS. after 24 h of exposure of complex **1** at 10, 20 μM，the uptake of copper element on DNA sample were 13.7 ng and 26.4 ng respectively, the results are shown in Fig. 4. This suggested that complex **1** could transported across the cellular phospholipid membrane, finally combined with DNA and then interact with DNA.

Apoptosis study by flow cytometry and confocal microscopy

To determine whether the observed cell death induced by the complexes was due to apoptosis or necrosis, the interaction of BEL-7404 cells with complex **1** was firstly investigated using an Annexin V-FITC/propidium iodide assay. As phosphatidylserine (PS) exposure usually precedes loss of plasma membrane integrity in apoptosis, the presence of annexin V^+/PI^- cells is considered an indicator of apoptosis. As shown in Fig. 5. , in the presence of complex **1**, the population of annexin V^+/PI^- cells (Q_4) was 40.5%, which suggested that apoptotic death was induced in BEL-7404 cells. On the basis of cell morphology and cell membrane integrity, normal, necrotic, and apoptotic cells can be distinguished by laser confocal microscopy. The apoptosis induction by complex **1** was further confirmed by DAPI/DiD staining assay. As shown in Fig. 6. , from which the characteristic morphological changes under the treatment of complex **1** can be observed, the nucleus of a living cell was stained as green fluorescence, and the red fluorescence represented the cell membrane. In the presence of complex **1**, the damage of the cell membrane and the apoptotic bodies of the nucleus were observed. These results indicated that the cell death induced by the complex **1** was mainly caused by the apoptotic pathway.

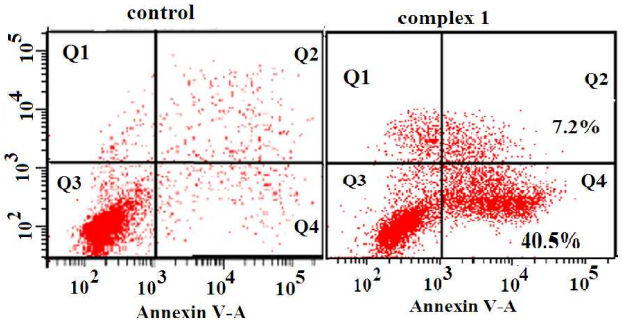

Fig. 5. AnnexinV/propidium iodide assay of BEL-7404 cells treated by complex **1** (at IC_{50} concentration) measured by flow cytometry.

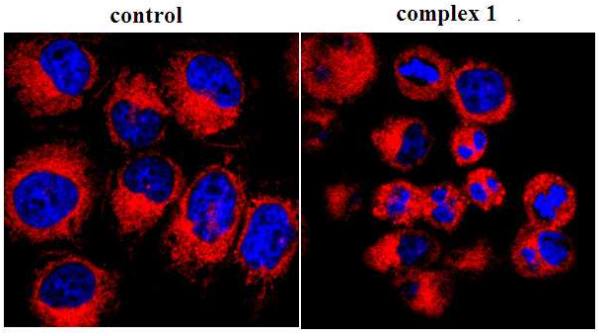

Fig. 6. DAPI/DiD assay of BEL-7404 cells treated by complex **1** (at IC_{50} concentration) measured by confocal microscope.

Cell cycle arrest

To determine whether the suppression of cancer cell growth by the complexes was caused by a cell cycle arrest. The BEL-7404 cells were treated with complex **1** at IC_{50} concentrations and the cell cycle phase was assayed through assessing the DNA content of cells stained with propidium iodide as measured by flow cytometry. As shown in Fig. 7., the complex **1** caused a raised-accumulation of BEL-7404 cells in the S phase, and the decrease of the accumulation were in the G0/G1 phase of the cell cycle. The cell population of S phase increased from 28.01% to 48.46% in the BEL-7404 cells, compared with the control, complex **1** induced drastic cell population decrease in G1 phase (from 65.43 % to 46.41 %) along with a concomitant accumulation in S phase in BEL-7404 cells. These results indicated remarkable S phase arrest. Actually, most DNA replication occurs within this stage, therefore it could be concluded that DNA may be one of the intracellular target for complex **1**.

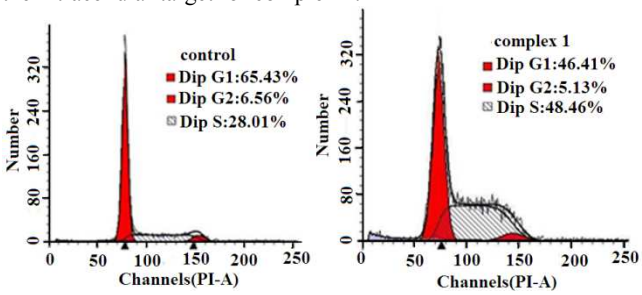

Fig. 7. Cell cycle analysis by flow cytometry for BEL-7404 cells treated with complex **1** .

Detection of mitochondrial membrane potential

Mitochondria act as a point of integration for apoptotic signals originating from both the extrinsic and intrinsic apoptotic

pathways. Mitochondrial dysfunction and the release of apoptogenic factors are critical events in triggering various apoptotic pathways. Loss of membrane potential is an important indicator of mitochondrial dysfunction. To delineate the importance of mitochondria in complex **1** induced BEL-7404 apoptosis, the variations in mitochondrial membrane potential were measured by the JC-1 probe, which was dispersed from aggregated form (red fluorescence) to the monomeric form (green fluorescence) when the mitochondrial membrane potential was lost. As shown in Fig. 8., the BEL-7404 cells treated with complex **1** exhibited a significant decrease in mitochondrial membrane potential as indicated by a notable shift in the ratio of green/red fluorescence versus control. The results suggested that mitochondria are involved in the process of apoptosis.

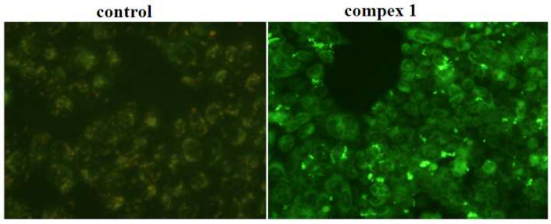

Fig. 8. Loss of $\Delta\Psi_m$ induced by complex **1**. Cells were treated with complex **1** for 0.5 h and examined by JC-1 under a fluorescence microscope.

Caspase-3 activation assay

It is well known that the caspase family plays a crucial role in the modulation of programmed cell death (PCD), which is a genetically regulated, evolutionarily conserved process with numerous links to many human diseases, most notably cancer. Caspase-3, the executioner caspase, is able to directly degrade multiple substrates including structural and regulatory proteins. Thus, therapeutic strategies designed to stimulate apoptosis by activating caspase-3 may combat cancer. Some small molecules have been shown to be selective activators of caspase-3, therefore, we have investigated whether the caspase-3 is activated when the BEL-7404 cells were exposed to complex **1**. As shown in Fig. 9., the BEL-7404 cells treated with complex **1** displayed a significant increase in the activity of caspase-3 as indicated by a notable shift in the ratio of green/dark fluorescence versus control. These results suggested that complex **1** could be an efficient activator of caspase-3.

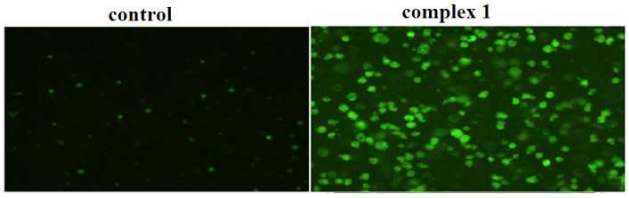

Fig. 9. the activation of caspase-3 induced by complex **1**, examined by FITC-DEVD-FMK under a fluorescence microscope.

The measurement of intrinsic pathway

The intrinsic pathway (via mitochondria) plays a key role in regulating apoptosis in response to various stimuli, beginning with the upregulation of wild-type p53 followed by the changes of Bcl-2 and Bax and so on, which increase the permeabilization of the mitochondrial outer membrane and then the mitochondria membrane potential could be changed, and that is also mediated by the release of cytochrome-c (Cyt-c), Ca^{2+} from mitochondria. Cyt-c then binds in complex with Apaf-1 and dATP, followed by activation of caspase-9 and caspase-3, then multiple substrates including structural and regulatory proteins are degraded and the apoptosis of cells happen.[44] The examination of mitochondria membrane potential and caspase-3 activation indicated that the intrinsic pathway are involved in the apoptotic process of BEL-7404 cells induced by complex **1**. To further confirm the intrinsic apoptotic pathway activated by complex **1**, we have analyzed the expression levels of a series of key proteins which are related with intrinsic pathway by means of Western blotting (see Fig. 10.). The studies showed that P53 proteins were up-regulated and Bcl-2 proteins have been down-regulated, at the same time, both caspase-9 and caspase-3 proteins were activated with the prolongation of time at 5 μM. The examination of four proteins further evidenced that the apoptosis of BEL-7404 cells induced by complex **1** were related with intrinsic pathway.

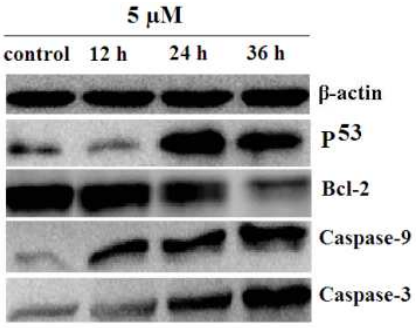

Fig. 10. Western blot analysis the expression of a series of proteins involved in mitochondria-mediated apoptosis after treatment with complex **1** for the indicated concentration and times.

DNA binding study

Despite the presence of other biological targets in tumor cells including RNA, enzyme and protein, it is generally accepted that DNA is the primary target for many metal-based anticancer drugs such as cisplatin.[45] Our previous work indicated that the metal complexes of isoquinoline alkaloids might act as bifunctional DNA-binding agents in which the isoquinoline ligand intercalates between the neighboring base pairs of DNA and the metal ions such as platinum(II) and zinc(II) covalently bind to DNA.[29-31] The ICP-MS and cell cycle arrest experiments have indicated that the DNA maybe one important target of complex **1**, in order to investigate the DNA binding properties of our newly synthesized isoquinoline copper complexes, a series of experiments exploring DNA binding were carried out, including DNA-melting analysis, fluorescence competitive binding, CD analysis, viscosity measurements and agarose gel electrophoresis assay.

DNA-melting analysis

The melting temperature (Tm) of DNA, which is defined as the temperature at which half of the dsDNA is dissociated into single strands, is strictly related to the stability of the macromolecule. In addition, the melting temperature of DNA may be altered by the interaction with chemicals. In general, the classic intercalation of small molecules into the double helix can increase the stability of the DNA helical structure and lead to the Tm of DNA increase 5–8 °C, while the non-intercalation binding causes no visible enhancement in Tm.[46] The melting curves of DNA and the DNA−compounds system are shown in Figs.11. and S2. As seen from the Figures, the Tm values of DNA in the absence and presence of the compounds were 71.97 °C, 75.03 °C (MPDQ),

80.26 °C (complex **1**), 77.10 °C (complex **2**) and 79.35 °C (complex **3**), respectively, indicating that the stability of DNA were increased in the presence of compounds. The Tm values of DNA in the presence of MPDQ only increased about 3.06 °C, in contrast, the Tm values of DNA can be more remarkably increase in copper(II) complexes solution, which strongly supported that the stronger intercalative binding of copper complexes to DNA have happened. Though, the Tm values of DNA in the presence of copper complexes have more obvious increase than MPDQ , the intercalative binding capacity of the copper(II) complexes were weaker than that of EtBr, because EB induced an increase in DNA Tm by 13 °C.[47]

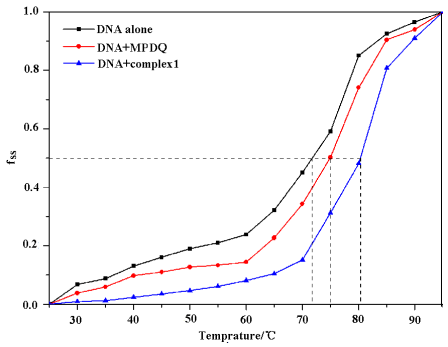

Fig. 11. The melting curves of DNA in the absence and presence of complex **1** and MPDQ.

Table 3 Calculated quenching ratios of EB by titration of complexes to EB-ctDNA system.

Complexes	One-step FI quenching ratio[a]	Total FI quenching ratio	K_q
Complex **1**	15.67%	72.55% at [complex **1**]/[EB]=8:1	0.33×10^4
Complex **2**	1.53%	18.37% at [complex **1**]/[EB]=8:1	0.11×10^3
Complex **3**	13.78%	66.74% at [complex **1**]/[EB]=8:1	0.27×10^4
MPDQ	0.52%	5.85% at [MPDQ]/[EB]=8:1	0.51×10^2

[a] FI, fluorescence intensity; one-step refers to [compound]/[EB]=1:1

Competitive binding study

The binding of all the present copper complexes and MPDQ to ct-DNA were investigated by a competing assay with ethidium bromide (EB) as an intercalative agent.[40] In the competitive binding experiments, the EB-ct-DNA system with [EB]/[DNA]=1:10 ([EB]=1×10^{-5} M, [DNA]=1×10^{-4} M) showed the characteristic strong emission at ca. 588 nm when excited at 332 nm, indicating that the intercalated EB molecules were sufficiently protected by the neighboring base pairs in the ct-DNA from being quenched by polar solvent molecules. When increasing the concentration of copper complexes from [compound]/[EB] = 1:1 to 8:1, the characteristic emission of EB were decreased, especially for copper(II) complexes **1** and **3** (as shown in Figs. 12. and S5). Table 3 lists the corresponding data of EB fluorescence quenching and the calculated competitive binding ability. It was found that all the complexes could quench the fluorescence emission of EB to a certain extent, which suggested that they may compete with EB to bind to ct-DNA through intercalation at the similar binding sites.[48] Furthermore, the quenching constant K_q was also calculated by restricted linear fitting of $[I_0/I]$ to [Q] from the Stern–Volmer equation and listed in Table 3. The results indicated that copper(II) complex **1** and **3** exhibited stronger quenching ability, but the complex **2** and ligand MPDQ were weaker.

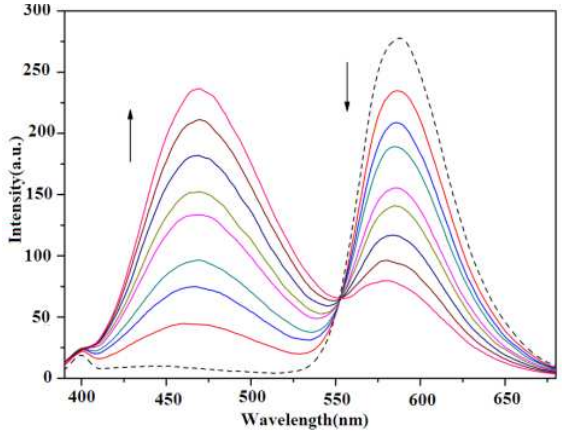

Fig. 12. Fluorescence emission spectra of EB bound with ct-DNA in the absence (dashed line ----) and presence (solid lines —) of complex **1** as competitive agent with increasing [complex **1**]/[EB] ratios of 1:1 to 8:1.

Circular dichroism (CD) analysis

Under the concentration of [DNA]/[compound] =10:1 to 10 :7, the presence of copper complex **1** induced obvious decrease on the positive and negative absorption of ct-DNA, which represents the intercalative binding of complex **1** with DNA (Fig.13).[49,50] At the same concentration, complexes **2**, **3** also induced significant changes on both the positive and negative absorption (Figs. S7/8), however, there were less variations in the CD characteristic DNA absorption peaks. These results indicated that all the complexes existed intercalative binding mode with DNA, but the intercalation of copper(II) complex **1** with DNA were still stronger than that of ligand MPDQ and complexes **2** and **3**.

Viscosity measurement studies

When small planar molecules intercalate into the neighboring base pairs of DNA, the DNA double helix loosens to the accommodate intercalation, resulting in a lengthening of the

DNA helix. Since the viscosity of the DNA solution is very sensitive to the changes in DNA length, the viscosity of the DNA solution is usually increased in the intercalation binding mode as the result of DNA length increase.[51]

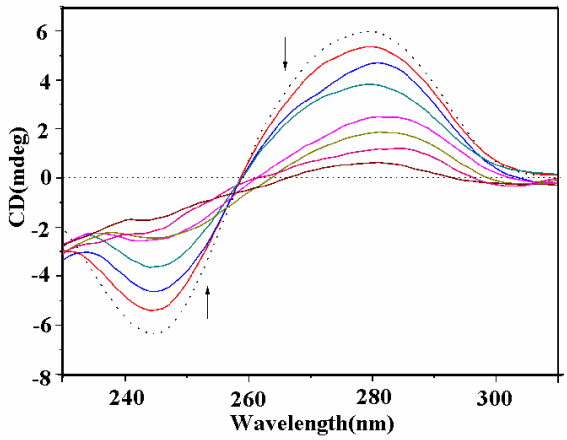

Fig. 13. Circular dichroism spectra of ct-DNA bound by complex **1** with [DNA]/[compound] ratios 2:1 to 7:1 (DNA alone of 1×10^{-4} M, dashed line; DNA bound by compounds, colored solid lines).

The influences of the binding of copper(II) complexes and MPDQ with ct-DNA on the viscosity of the ct-DNA solution are shown in Fig. 14., in which EtBr was employed as the intercalative binding indicator. The addition of MPDQ resulted in an increase on the viscosity of DNA solution but to a very slight extent, the DNA viscosity only increased about 8.1% as the [MPDQ]/[DNA] ratio increased from 0.02 to 0.20, in contrast, as the [copper(II) complexes]/[DNA] ratio increased from 0.02 to 0.20, the all viscosity of DNA solution have a more obvious increase than MPDQ, basing on the above results, the intercalative binding mode exists between the copper(II) complexes and ct-DNA could be concluded, furthermore, the complex **1** induced the greatest viscosity increase in ct-DNA solutions in all copper(II) complexes. Nevertheless, the intercalative binding capacity of the copper(II) complex **1** was still somewhat weaker than that of EtBr. EtBr induced an increase in DNA viscosity by 24.81% at the [EtBr]/[DNA] ratio of only 0.14 : 1.[52]

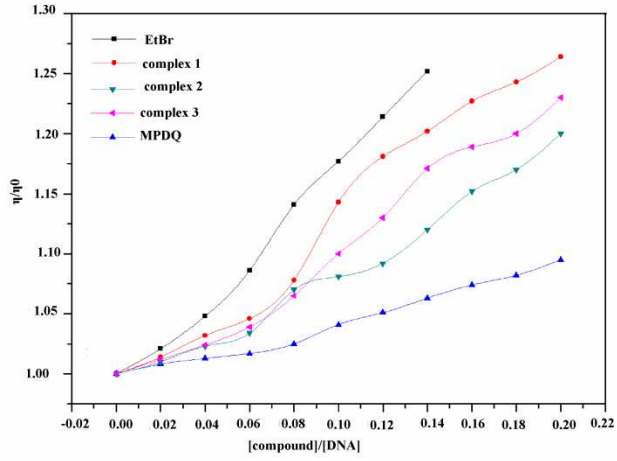

Fig. 14. Relative viscosity of ct-DNA solution bound with copper(II) complexes and MPDQ with increasing [compound]/[DNA] ratios in the range from 0.02 to 0.20. EtBr as intercalative indicator was set for comparison.

In summary, the DNA binding studies revealed that the binding mode of the copper(II) complexes with ct-DNA were mainly through intercalation, which was supported by the results from DNA-melting, competitive binding, CD and viscosity measurements. The copper(II) complexes induced more significant changes in the all spectra of ct-DNA than that of free MPDQ, which may be result from the increased planarity of the complexes after MPDQ coordinated to copper (II) ions, and the copper(II) ion in nature. The DNA binding ability of copper(II) complexes to ct-DNA could be correlated to their antitumor activity.

Conclusions

Three new copper(II) complexes of 4,5-methylenedioxy-1-pyridinedihydroisoquinoline were synthesized and fully characterized. These dihydroisoquinoline-copper(II) complexes exhibited enhanced cytotoxicity against tested human tumor cell lines comparing to free MPDQ and corresponding copper(II) salts, suggesting synergistic effect between MPDQ and copper(II) ions, and displayed selective cytotoxicity to the tested tumor cells. Complex **1** can induce BEL-7404's apoptotic death by triggering S phase cell cycle arrest, moreover, mitochondria membrane potential and caspase-3 activation assay indicated that the pathway of apoptosis induced by complex **1** correlated the intrinsic pathway of mitochondria. The results were further confirmed by analyzing the key proteins of mitochondria pathway. ICP-MS testing indicated that complex **1** could enter cells and interact with DNA of nucleus. The most possible binding mode of copper(II) complexes with ct-DNA might be the intercalation by the DNA binding assays.

Acknowledgements

This work was supported by the National Natural Science Foundation of China (Nos. 21271051, 21401031, 21431001, 81473102), National Basic Research Program of China (No. 2012CB723501), IRT1225, and Natural Science Foundation of Guangxi Province (Nos.2014GXNSFBA118035) as well as "BAGUI Scholar" program of Guangxi, China.

Notes and References

[a] *Guangxi Key Laboratory for the Chemistry and Molecular Engineering of Medicinal Resources, School of Chemistry and Pharmacy of Guangxi Normal University, Guilin 541004, P. R. China. E-mail address: chenzf@gxnu.edu.cn (Z.–F. Chen), hliang@gxnu.edu.cn (H. Liang), Tel./Fax: +86-773-2120958 (Z.–F. Chen).*

[b] *School of Chemistry of Nankai University, Tianjin 300071, P. R. China.*

† Electronic supplementary information (ESI) available. Crystallographic data for the structural analysis have been deposited with the Cambridge Crystallographic Data Centre, CCDC Nos. 923488-923490 for complexes **1–3**. The data can be obtained free of charge via http://www.ccdc.cam.ac.uk, or from the Cambridge Crystallographic Data Centre, 12 Union Road, Cambridge CB21EZ, UK; fax: (+44) 1223-336-033; or e-mail:deposit@ccdc.cam.ac.uk.

1 Y. Jung, S. J. Lippard, Chem. Rev., 2007, **107**, 1387-1407.
2 J. J. Wilson, S. J. Lippard, J. Med. Chem., 2012, **55**, 5326-5336.
3 E. Wexselblatt, D. Gibson, J. Inorg. Biochem., 2012, **117**, 220-229.

4 C. P. Tan, S. S. Lai, S. H. Wu, S. Hu, L. J. Zhou, Y. Chen, M. X. Wang, Y. P. Zhu, W. Lian, W. L. Peng, L. N. Ji, and A. L. Xu, J. Med. Chem., 2010, **53**, 7613-7624.

5 B. M. Zeglis, V. Divilov, and J. S. Lewis, J. Med. Chem., 2011, **54**, 2391-2398.

6 Z.-F. Chen, Y. Q. Gu, X. Y. Song, Y. C. Liu, Y. Peng, H. Liang, Eur. J. Med. Chem., 2013, **59**, 194-202.

7 Z.-F. Chen, Y.-F. Shi, Y.-C. Liu, X. Hong, B. Geng, Y. Peng, and H. Liang, Inorg. Chem., 2012, **51**, 1998-2009.

8 I. Bratsos, T. Gianferrara, E. Alessio, C. G. Hartinger, M. A. Jakupec, B. K. Keppler, Bioinorg. Med. Chem., 2011, 151-174.

9 M. E. Bravo-Gomez, L. Ruiz-Azuara, Edited by M. D. C. Mejia Vazquez, S. Navarro, New approaches in the treatment of cancer, 2010, 139-172.

10 M. F. Primik, S. Goschl, M. A. Jakupec, A. Roller, B. K. Keppler, and V. B. Arion, Inorg. Chem., 2010, **49**, 11084-11095.

11 H. Thomadaki, A. Karaliota, C. Litos, and A. Scorilas, J. Med. Chem., 2008, **51**, 3713-3719.

12 C. Duncan, A. R. White, Metallomics, 2012, **4**, 127-138.

13 M. Porchia, A. Dolmella, V. Gandin, C. Marzano, M. Pellei, V. Peruzzo, F. Refosco, C. O. Santini, F. Tisato, Eur. J. Med. Chem., 2013, **59**, 218-226.

14 M. Connor, A. Kellett, M. M. Cann, G. Rosair, M. M. Namara, O. Howe, B. S. Creaven, S. M. Clean, A. F. A. Kia, D. O'Shea, and M. Devereux, J. Med. Chem., 2012, **55**, 1957-1968.

15 G. Murtaza, M. K. Rauf, A. Badshah, M. Ebihara, M. Said, M. Gielen, D. Vosd, E. Dilshad, B. Mirza, Eur. J. Med. Chem., 2012, **48**, 26-35.

16 S. Tardito, A. Barilli, I. Bassnetti, M. Tegoni, O. Bussolati, R. Franchi-Gazzola, C. Mucchino, L. Marchio, J. Med. Chem., 2012, **55**, 10448-10459.

17 D. Palanimuthu, S. V. Shinde, K. Somasundaram, A. G. Samuelson, J. Med. Chem., 2013, **56**, 722-730.

18 K. Somdej, K. Kwanjai, L. Ratsami, J. Nat. Prod., 2007, **70**, 1536-1536-1538.

19 D. Cappoen, J. Jacobs, T. N. Van, S. Claessens, G. Diels, R. Anthonissen, T. Einarsdottir, M. Fauville, L. Verschaeve, K. Huygen, N. D. Kimpe, Eur. J. Med. Chem., 2012, **48**, 57-68.

20 B. Gerhard, Z. Guoliang, B. Tobias, B. Gabi, K. Thomas, B. Holger, B. Reto, M. Virima, Chem. Eur. J., 2013, 916-923.

21 A. Bermejo, I. Andreu, F. Suvire, S. LeÂonce, D. H. Caignard, P. Renard, A. Pierrea, R. D. Enriz, D. Cortes, N. Cabedo, J. Med. Chem., 2002, **45**, 5058-5068.

22 S. A. Kim, Y. Kwon, J. H. Kim, M. T. Muller, I. K. Chung, Biochemistry, 1998, **37**, 16316-16324.

23 M. Goldbrunner, G. Loidl, T. Polossek, A. Mannschreck, E. Von Angerer, J. Med. Chem.,1997, **40**, 3524-3533.

24 W. J. Houlihan, S. H. Cheon, V. A. Parrino, D. A. Handley, D. A. Larson, J. Med. Chem., 1995, **36**, 234-240.

25 D. Colangelo, A. L. Ghiglia, I. Viano, G. Cavigiolio, D. Osella, Biometals, 2003, **16**, 553-560.

26 U. Bierbach, Y. Qu, T. W. Hambley, J. Peroutka, H. L. Nguyen, M. Doedee, N. Farrell. Inorg. Chem., 1999, **38**, 3535-3536.

27 E. S. F. Ma, W. D. Bates, A. Edmunds, L. R. Kelland, T. Fojo, N. Farrell, J. Med. Chem., 2005, **48**, 5651-5654.

28 F. Nussbaum, B. Miller, S. Wild, C. S. Hilger, S. Schumann, H. Zorbas, W. Beck, W. Steglich, J. Med. Chem., 1999, **42**, 3478-3485.

29 Z.-F. Chen, Y.-C. Liu, L.-M. Liu, H.-S. Wang, S.-H. Qin, B.-L. Wang, H.-D. Bian, B. Yang, H.-K. Fun, H.-G. Liu, H. Liang, C. Orvig, Dalton Trans., 2009, 262-272.

30 Y.-C. Liu, Z.-F. Chen, L.-M. Liu, Y. Peng, X. Hong, B. Yang, H.-G. Liu, H. Liang and C. Orvig, Dalton Trans. 2009, 10813-10823.

31 Z.-F. Chen, Y.-C. Liu, Y. Peng, X. Hong, H. H. Wang, M.-M. Zhang, H. Liang, J. Biol. Inorg. Chem., 2012, **17**, 247-261.

32 R. Al, J. Adnan, C.-Y. Gao, G. E. Martin, F.T. Lin, M. A. Zemaitis, P. L. Schiff, Planta Med., 1998, **64**, 681.

33 A. Bermejo, I. Andreu, F. Suvire, S. Leonce, D. H. Caignard, P. Renard, A. Pierre, R. D. Enriz, D. Cortes, N. Cabedo, J. Med. Chem., 2002, **45**, 5058-5068.

34 C.-H. Zheng, J. Chen, J. Liu, X.-T. Zhou, N. Liu, D. Shi, J.-J. Huang, J.-G. Lv, J. Zhu, Y.-J. Zhou, Arch. Pharm. Chem. Life Sci., 2012, **345**, 454-458.

35 Y. Zhang, J. Feng, C. Liu, L. Zhang, J. Jiao, H. Fang, L. Su, X. Zhang, J. Zhang, M. Li, B. Wang, W. Xu, Bioorg. Med. Chem., 2010, **18**, 1761-1772.

36 K.-B. Huang, H.-Y. Mo, J.-H. Wei, Y.-C. Liu, Z.-F. Chen, H. Liang, Eur. J. Med. Chem., 2015, **100**, 5213-5222.

37 K.-B. Huang, Z.-F. Chen, Y.-C. Liu, M. Wang, J.-H. Wei, X.-L. Xie, J.-L. Zhang, K. Hu, H. Liang, Eur. J. Med. Chem., 2013, **70**, 640-648.

38 G. M. Sheldrick, Phase Annealing in SHELXL-90: Direct methods for larger structures, Acta Crystallogr. A., 1990, **46**, 467.

39 G. M. Sheldrick, SHELXS-97, Program for X-ray crystal structure Solution, University of Göttingen: Göttingen, Germany, 1997.

40 K.-B. Huang, Z.-F. Chen, Y.-C. Liu, Z.-Q. Li, J.-H. Wei, M. Wang, G.-H. Zhang, H. Liang, Eur. J. Med. Chem., 2013, **63**, 76-84.

41 P. Zhao, J. W. Huang, W. J. Mei, J. He, L. N. Ji, Spectrochim. Acta, Part A., 2010, **75**, 1108-1114.

42 M. C. Alley, D. A. Scudiero, A. Monks, M. L. Hursey, M. J. Czerwinski, D. L. Fine, B. J. Abbott, J. G. Mayo, R. H. Shoemaker, M. R. Boyd, Cancer Res., 1988, **48**, 589-592.

43 P. U. Maheswari, S. Barends, S. O. Yaman, P. de Hoog, H. Casellas, S. J. Teat, C. Massera, M. Lutz, A. L. Spek, G. P. v. Wezel, P. Gamez, and J. Reedijk. Chem. Eur. J. 2007, **13**, 5213-5222.

44 H. Wang, H. Liu, Z. M. Zheng, K. B. Zhang, T. P. Wang S. S. Sribastav, W. S. Liu, T. Liu. Apoptosis, 2011, **16**, 990-1003.

45 Y. Barenholz, J. Kasparkova, V. Brabec, D. Gibson, Angew. Chem. Int. Ed., 2005, **44**, 2885-2887.

46 S. Kashanian, M. M. Khodaei, P. Pakravan, Cell Biol., 2010, **29**, 639-646.

47 M. Cory, D. D. Mckee, J. Kagan, D.W. Henry, J. A. Miller, J. Am. Chem. Soc., 1985, **107**, 2528-2536.

48 G. H. Clever, Y. Söltl, H. Burks, W. Spahl, T. Carell, Chem. Eur. J., 2006, **12**, 8708-8718.

49 V. Rajendiran, M. Murali, E. Suresh, M. Palaniandavar, V. S. Periasamy, M. A. Akbarsha. Dalton Trans. 2008, 2157-2170.

50 S. Schäfe, I. R. Ott Gust, W. S. Sheldrick, Eur. J. Inorg. Chem., 2007, 3034.

51 C. Rajput, R. Rutkaite, L. Swanson, I. Haq, J. A. Thomas, Chem. Eur. J., 2006, **12**, 3034-3046.

52 P. G. Baraldi, A. Bovero, F. Fruttarolo, D. Preti, M. A. Tabrizi, M. G. Pavani, R. Romagnoli, Med. Res. Rev. 2004, **24**, 475-528.

Dihydroisoquinoline Copper(II) Complexes: Crystal Structures, Cytotoxicity, and Their Action Mechanism

Ke-Bin Huang, Zhen-Feng Chen, Yan-Cheng Liu, Xiao-Li Xie, and Hong Liang

Three new copper(II) complexes with dihydroisoquinoline were synthesized. They exhibited considerable cytotoxicity achieved through the induction of cell apoptosis via the intrinsic pathways of caspase–mitochondria.